International Journal of Modern Physics D
Vol. 20, No. 13 (2011) 2471–2496

DOI: 10.1142/S0218271811020469

BORN–INFELD BLACK HOLES COUPLED TO A MASSIVE SCALAR FIELD

DANIELA A. GEORGIEVA[*,§], IVAN ZH. STEFANOV[†,¶], STOYTCHO S. YAZADJIEV[‡,‖] and MICHAIL D. TODOROV[*,**]

[*]*Faculty of Applied Mathematics and Computer Science, Technical University of Sofia, 8, Kliment Ohridski Boulevard, 1000 Sofia, Bulgaria*

[†]*Department of Applied Physics, Technical University of Sofia, 8, Kliment Ohridski Boulevard, 1000 Sofia, Bulgaria*

[‡]*Department of Theoretical Physics, Faculty of Physics, St. Kliment Ohridski University of Sofia, 5, James Bourchier Boulevard, 1164 Sofia, Bulgaria*

[§]*dgeorgieva@tu-sofia.bg*
[¶]*izhivkov@tu-sofia.bg*
[‖]*yazad@phys.uni-sofia.bg*
[**]*mtod@tu-sofia.bg*

Received 5 May 2011
Revised 23 August 2011

Born–Infeld black holes in the scalar–tensor theories of gravity with massless scalar field have been recently obtained [I. Stefanov, S. Yazadjiev and M. Todorov, *Phys. Rev. D* **75** (2007) 084036; *Mod. Phys. Lett. A*. **23**(34) (2008) 2915; *Class. Quantum Gravity* **26** (2009) 015006]. The aim of the current paper is to study the effect of the inclusion of a potential for the scalar field in the theory, through a combination of analytical techniques and numerical methods. The black holes coupled to a massive scalar field have richer causal structure in comparison to the massless scalar field case. In the former case, the black holes may have a second, inner horizon. The presence of potential for the scalar field allows the existence of extremal black holes for certain values of the mass of the scalar field and the magnetic (electric) charge of the black hole. The solutions are stable against spherically symmetric perturbations. Arguments in favor of the general stability of the solutions coming from the application of the "turning point" method are also presented.

Keywords: Scalar–tensor theories of gravity; nonlinear electrodynamics; black holes; stability; thermodynamics.

1. Introduction

The study of black holes coupled to nonlinear electrodynamics is natural since in the conditions of strong fields and strong sources, such as black holes, quantum corrections to the Lagrangian of electrodynamics should be taken into account. Nonlinear electrodynamics was considered for the first time by Born and Infeld in

1934 in their attempt to obtain a finite energy density model for the electron.[1] The interest in electrodynamics with nonlinear Lagrangians has been recently revived since such types of Lagrangians appear in the low-energy limit of open strings and D-branes.[2–5] Nonlinear electrodynamicsmodels coupled to gravity have been discussed in different aspects (see, for example, Refs. 6–23 and references therein).

The properties of charged black holes in the Einstein–Born–Infeld (EBI) theory have been examined in Refs. 10 and 24–26, and in the case of nonzero cosmological constant in Ref. 27. The role of the derivative corrections to the properties of the EBI black holes have been studied in Ref. 28. A natural step in the study of charged black holes is to add a scalar field in the theory. Born–Infeld-dilaton black holes, both asymptotically flat and asymptotically nonflat, have been reported in Refs. 29–36. The case of charged black holes with massivedilaton coupled to abelian gauge field with linear Lagrangian have been considered in Refs. 37–39. EBI black holes with massive dilaton have also been investigated (see Ref. 43).[a]

In the frame of scalar–tensor theories (STTs) solutions describing charged black holes with nontrivial massless scalar field in nonlinear electrodynamics have been recently obtained.[41–43] The aim of the current paper is to extend the results of Refs. 41 and 43 by adding a potential for the scalar field that admits the presence of asymptotically flat black holes.

The solutions with massless scalar field presented in Refs. 41 and 43 have a much simpler causal structure than the corresponding solutions in the EBI theory. The former have a single horizon, thus their structure resembles that of the Schwarzschild solution. Adding a potential for the scalar field makes the causal structure richer and more difficult to study. In that case, solutions with internal horizons and with degenerate event horizons may appear.

A prior intuition about the properties of the studied solutions could be obtained from other similar systems that have already been studied. An example of such systems are the charged black holes with massive dilaton coupled to linear electrodynamics. Not all techniques used in that system are applicable to our case, though. The major difference between the dilaton and the gravitational scalar in the STTs is its coupling to matter,[b] and in particular, to the electromagnetic field. In STTs due to the specific coupling between the scalar and electromagnetic fields, the source term in the field equation for the scalar field is proportional to the trace of the energy–momentum tensor of the electromagnetic field and not proportional to the Lagrangian of the electromagnetic field as it is in the dilaton gravity.

The charged black holes with massive dilaton have been studied analytically in Ref. 37 and numerical solutions have been obtained in Ref. 38. In Ref. 37, the

[a]This model studied in Ref. 40 should not be confused with the model considered in the current paper. Some clarifying remarks on the difference between the scalar field of the STT and the dilaton can be found further in Sec. 1.

[b]The coupling between the electromagnetic field and the scalar field in dilaton gravity and in STT is different. The difference between the two types of actions can be found, for example, in Ref. 44.

conclusions about the causal structure are made. In that case black holes may have three, two or one horizon(s) depending on the values of the parameters and the specific choice for the potential of the dilaton. The various types of extremal solutions were also studied. The authors found that two-fold and three-fold degenerate horizons may exist. The behavior of the fields near the central singularity was also obtained in that paper. In Ref. 38, approximate solution in the two limiting cases — large black holes (with radius of the event horizon much bigger than the Compton length of the dilaton) and small black holes (with radius of the event horizon much smaller than the Compton length of the dilaton) — have been obtained. Numerical solutions covering both the exterior and interior regions of the black holes are also presented.

In the current paper, our aim is to study the black holes solutions in a class of STT with massive scalar field coupled to Born–Infeld nonlinear electrodynamics. In the studied region of the parameter space, we exclude the possibility of the existence of a third horizon. We also study the possibility for existence of extremal black holes in different regions of the parameter space and obtain numerical solutions for them in the allowed region.

In the present paper, we have commented also on the linear stability of the obtained black-hole solutions against radial perturbations. Here we follow the same scheme as for the black holes with massless scalar field.[43] Additional arguments in favor of the general stability of the black holes can be also given on the basis of the "turning point" method that we discuss.

2. Formulation of the Problem

The action of the studied STT is originally formulated in the so-called Jordan frame in which the scalar field is coupled to the scalar curvature and in which there is no direct coupling between the scalar field and the sources of gravity (here the source of gravity is the electromagnetic field). For mathematical convenience, however, as usual for the STT, we study the solutions in the conformally related Einstein frame (for more details we refer the reader to Refs. 41, 45 and 46). In the Einstein frame, the action takes the following form:

$$S = \frac{1}{16\pi G_*}\int d^4x\sqrt{-g}[\mathcal{R} - 2g^{\mu\nu}\partial_\mu\varphi\partial_\nu\varphi - 4V(\varphi)] + S_m[\Psi_m; \mathcal{A}^2(\varphi)g_{\mu\nu}], \quad (1)$$

where $\mathcal{R}$ is the Ricci scalar curvature with respect to the Einstein metric $g_{\mu\nu}$ and G_* is the bare gravitational constant. $\mathcal{A}(\varphi)$ which occurs in the material sector of the action is a function which determines the coupling between the scalar field and the material fields, the electromagnetic field in particular. $V(\varphi)$ is the potential of the scalar field. The type of STT is determined by the specific explicit form of the functions $\mathcal{A}(\varphi)$ and $V(\varphi)$.

The action of the nonlinear electrodynamics is

$$S_m = \frac{1}{4\pi G_*}\int d^4x\sqrt{-g}\mathcal{A}^4(\varphi)L(X, Y), \quad (2)$$

where

$$X = \frac{\mathcal{A}^{-4}(\varphi)}{4} F_{\mu\nu} g^{\mu\alpha} g^{\nu\beta} F_{\alpha\beta}, \quad Y = \frac{\mathcal{A}^{-4}(\varphi)}{4} F_{\mu\nu} (\star F)^{\mu\nu}, \tag{3}$$

and "$\star$" stands for the Hodge dual with respect to the Einstein frame metric $g_{\mu\nu}$.

The action (1) with (2) yields the following field equations

$$\begin{aligned} \mathcal{R}_{\mu\nu} &= 2\partial_\mu\varphi\partial_\nu\varphi + 2V(\varphi)g_{\mu\nu} - 2\partial_X L(X,Y)\left(F_{\mu\beta}F^{\beta}_{\nu} - \frac{1}{2}g_{\mu\nu}F_{\alpha\beta}F^{\alpha\beta}\right) \\ &\quad -2\mathcal{A}^4(\varphi)[L(X,Y) - Y\partial_Y L(X,Y)]g_{\mu\nu}, \\ &\quad \nabla_\mu[\partial_X L(X,Y)F^{\mu\nu} + \partial_Y L(X,Y)(\star F)^{\mu\nu}] = 0, \\ \nabla_\mu\nabla^\mu\varphi &= \frac{dV(\varphi)}{d\varphi} - 4\alpha(\varphi)\mathcal{A}^4(\varphi)[L(X,Y) - X\partial_X L(X,Y) - Y\partial_Y L(X,Y)], \end{aligned} \tag{4}$$

where $\alpha(\varphi) = d\ln\mathcal{A}(\varphi)/d\varphi$.

In what follows, we consider the truncated[c] Born–Infeld electrodynamics described by the Lagrangian

$$L_{BI}(X) = 2b\left(1 - \sqrt{1 + \frac{X}{b}}\right). \tag{5}$$

The parameter b is usually referred to as the Born–Infeld parameter and is inversely proportional to the string tension. In the limit $b \to \infty$, the Born–Infeld Lagrangian restores the Maxwell electrodynamics.

Here, we will restrict our study to potentials $V(\varphi)$ which satisfy the conditions

$$\varphi\frac{dV(\varphi)}{d\varphi} \geq 0 \quad \text{and} \quad \frac{dV(\varphi=0)}{d\varphi} = 0. \tag{6}$$

In particular, for numerical calculations, we will choose the potential of the scalar field in the form

$$V(\varphi) = \frac{1}{2}m_*^2\varphi^2, \tag{7}$$

where m_* is the mass of the scalar field and has also the meaning of inverse-Compton wavelength of the scalar field in the units we work. Constraints for the values of m_* can be found in Ref. 47.

In the present paper, we will be searching for solutions with regular scalar field φ on the event horizon. We will also require that $0 < \mathcal{A}(\varphi) < \infty$ for $r \geq r_H$, where r_H is the radius of the horizon in order to ensure the regularity of the transition between the Einstein and the Jordan conformal frames. Yet, we will consider only theories for which $\alpha(\varphi)$ has a fixed positive sign for all values of φ. The manner of investigation of solutions within theories with $\alpha(\varphi) < 0$ is similar. Theories

[c]Here we consider the pure magnetic case for which $Y = 0$.

in which the coupling function changes its sign are much more complicated (also from numerical point of view) since some interesting nonperturbative effects like "spontaneous scalarization" may appear in them, especially when $\alpha(\varphi) \sim \varphi$ (see Ref. 42).

For our numerical solution, we have considered theories for which the coupling function has the form

$$\mathcal{A}(\varphi) = e^{\alpha\varphi}, \tag{8}$$

where α is a positive constant and in this theory $\alpha(\varphi) = \text{const.} \equiv \alpha$. We have studied the parametric space for fixed value of the coupling parameter $\alpha = 0.01$. The conclusions for the qualitative behavior of the solutions, however, are valid for a much wider class of STT for which $\alpha(\varphi) > 0$, $\alpha(\varphi = 0) \sim 10^{-4} \div 10^{-2}$ and $\beta(\varphi = 0) > -4.5$ (such values are in agreement with the observational constraints, for details see Ref. 48), where $\beta(\varphi) = d\alpha(\varphi)/d\varphi$. The exterior region solutions in that class of STTs would not only be qualitatively the same but also quantitatively very close to the exterior region solutions in the Brans–Dicke theory since, as the numerical results show, φ is very small there and higher-order (in φ) terms in the coupling function would have negligible contribution.

3. Basic Equations

3.1. *The reduced system*

In the present paper, we will be searching for static, spherically symmetric, asymptotically flat black holes. The metric of a static, spherically symmetric spacetime can be written in the form

$$ds^2 = g_{\mu\nu}dx^\mu dx^\nu = -f(r)e^{-2\delta(r)}dt^2 + \frac{dr^2}{f(r)} + r^2(d\theta^2 + \sin^2\theta d\phi^2), \tag{9}$$

where

$$f(r) = 1 - \frac{2m(r)}{r}. \tag{10}$$

$m(r)$ is the so-called local gravitational mass and should not be confused with the mass of the scalar field m_*. We will study the magnetically charged black holes for which the electromagnetic field strength is given by

$$F = P\sin\theta d\theta \wedge d\phi \tag{11}$$

and the magnetic charge is denoted by P. The electrically charged solutions can be obtained through electric–magnetic duality rotations (we refer the reader to Refs. 10, 11, 15 and 43 for more details on these duality transformations) of the type

$$\{g_{\mu\nu}, \varphi, F_{\mu\nu}, P, X, L(X)\} \leftrightarrow \{g_{\mu\nu}, \varphi, \star G_{\mu\nu}, \bar{Q}, \bar{X}, L(\bar{X})\}. \tag{12}$$

The barred quantities are related to the dual system. Here

$$G_{\mu\nu} = -2\frac{\partial[\mathcal{A}^4(\varphi)L]}{\partial F^{\mu\nu}}, \tag{13}$$

$$\bar{X} = -[\partial_X L(X)]^2 X, \tag{14}$$

and $\bar{Q}$ is the electric charge of the dual solution. The Born–Infeld Lagrangian (5) belongs to the class of Lagrangians for which the system (4) is invariant under the electric–magnetic duality transformations (12). As a consequence of that invariance, the solutions for the metric functions and the scalar field in the electrically charged case and the magnetically charged case coincide.

The field equations reduce to the following coupled system of ordinary differential equations

$$f'' - 2f\delta'' - 3f'\delta' + 2f\delta'^2 + \frac{2}{r}f' - \frac{4}{r}f\delta' = -4\{V(\varphi) + \mathcal{A}^4(\varphi)[2X\partial_X L(X) - L(X)]\}, \tag{15}$$

$$f'' - 2f\delta'' - 3f'\delta' + 2f\delta'^2 + \frac{2}{r}f' = -4\{f\varphi'^2 + V(\varphi) + \mathcal{A}^4(\varphi)[2X\partial_X L(X) - L(X)]\}, \tag{16}$$

$$1 - f - rf' + rf\delta' = 2r^2[V(\varphi) - \mathcal{A}(\varphi)^4 L(X)], \tag{17}$$

$$\frac{d}{dr}\left(e^{-\delta}r^2 f\frac{d\varphi}{dr}\right) = \frac{dV(\varphi)}{d\varphi}r^2 + 4r^2 e^{-\delta}\alpha(\varphi)\mathcal{A}^4(\varphi)[X\partial_X L(X) - L(X)], \tag{18}$$

where X reduces to

$$X = \frac{\mathcal{A}^{-4}(\varphi)}{2}\frac{P^2}{r^4}. \tag{19}$$

It is a system of four equations for three unknown functions but, as it is well known, the self-consistency of the system is guaranteed by the Bianchi identity. For numerical treatment of the problem, however, the following form is more convenient

$$\frac{d\delta}{dr} = -r\left(\frac{d\varphi}{dr}\right)^2, \tag{20}$$

$$\frac{dm}{dr} = r^2\left[\frac{1}{2}f\left(\frac{d\varphi}{dr}\right)^2 + V(\varphi) - \mathcal{A}(\varphi)^4 L(X)\right], \tag{21}$$

$$\frac{d}{dr}\left(r^2 f\frac{d\varphi}{dr}\right) = r^2\left\{\frac{dV}{d\varphi} - 4\alpha(\varphi)\mathcal{A}^4(\varphi)[L - X\partial_X L(X)] - rf\left(\frac{d\varphi}{dr}\right)^3\right\}. \tag{22}$$

In this form the last two equations are separated as an independent sub-system.

3.2. *Qualitative investigation*

Some general properties of the solutions can be derived through an analytical investigation of the equations. The major difference resulting from the different type of coupling between the scalar field and the electromagnetic field is as follows. In both theories, STT and dilaton gravity, the right-hand side (RHS) of some of the generalized Einstein equations for the metric functions is proportional to the Lagrangian of the electromagnetic field. The RHS of the equation for the scalar field in STT is proportional to the trace of the energy–momentum tensor of the electromagnetic field, while in dilaton gravity it is proportional to the Lagrangian of the electromagnetic field. The last fact allows in the case of dilaton gravity combinations between the field equations which are favorable for the analytical investigation of the properties of the solutions to be made.

Analytical assessments and results though not very complete are always welcome since the entire space of parameters cannot be thoroughly examined via numerical methods. The examination of the properties of the solutions is additionally impeded by the presence of numerical instabilities for some values of the parameters. Such instabilities appear especially in the interior region and have been reported also in Ref. 38.

For our assessments, we will use the fact that for the Born–Infeld Lagrangian of nonlinear electrodynamics (5) the relations

$$X\partial_X L(X) - L(X) > 0 \quad \text{and} \quad 2X\partial_X L(X) - L(X) < 0 \tag{23}$$

hold.

For the analytical treatment we will also use the boundary conditions presented in Sec. 5.

It can be proved that $\varphi(r)$ is nonpositive outside the event horizon. Let us first exclude the possibility that $\varphi(r)$ is positive on the event horizon.

Proposition 1. *$\varphi(r)$ cannot be positive on the event horizon.*

Proof. In order to prove this we will use Eq. (18). Let us admit that $\varphi(r)$ is positive on the event horizon and has one or more roots in the exterior region. Then we multiply Eq. (18) by $\varphi(r)$ and integrate it in the interval $r \in [r_H, r_0]$ where we denote the radius of the event horizon by r_H and the leftmost zero of $\varphi(r)$ which is to the right of r_H by r_0

$$\int_{r_H}^{r_0} \varphi \frac{d}{dr}\left(e^{-\delta} r^2 f \frac{d\varphi}{dr}\right) dr = \int_{r_H}^{r_0} \left\{\varphi \frac{dV(\varphi)}{d\varphi} r^2 + 4r^2 e^{-\delta} \varphi \alpha(\varphi) \mathcal{A}^4(\varphi)[X\partial_X L(X) - L(X)]\right\} dr. \tag{24}$$

After integrating by parts we get

$$\left(\varphi e^{-\delta} r^2 f \frac{d\varphi}{dr}\right)\Big|_{r_0} - \left(\varphi e^{-\delta} r^2 f \frac{d\varphi}{dr}\right)\Big|_{r_H} - \int_{r_H}^{r_0} \left[e^{-\delta} r^2 f \left(\frac{d\varphi}{dr}\right)^2\right] dr$$

$$= -\int_{r_H}^{r_0} \left[e^{-\delta} r^2 f \left(\frac{d\varphi}{dr}\right)^2\right] dr$$

$$= \int_{r_H}^{r_0} \left\{\varphi \frac{dV(\varphi)}{d\varphi} r^2 + 4r^2 e^{-\delta} \varphi \alpha(\varphi) \mathcal{A}^4(\varphi)[X\partial_X L(X) - L(X)]\right\} dr. \quad (25)$$

Taking into account (6) and (23) and the fact that according to the admission φ is positive in $r \in [r_H, r_0]$, we see that the sign of the RHS of (25) is positive. The left-hand side (LHS), however, is negative since $f(r) > 0$ outside the event horizon. The contradiction we reach means that our admission is incorrect. If we admit that $\varphi(r)$ is positive on the event horizon and has no roots following the same procedure we will again reach a contradiction. In order to see this, it is enough to let $r_0 \to \infty$ in (24) and to impose the boundary condition $\varphi(r) \to 0$ at infinity. □

Proposition 2. *Function $\varphi(r)$ is negative and has no zeros in the exterior region.*

Proof. Let us admit that $\varphi(r)$ has zeros. We already know that $\varphi(r)$ is negative on the event horizon and also require it to satisfy the vanishing boundary conditions at infinity. Then one of the following two situations must be realized. Either $\varphi(r)$ has at least one positive maximum or it has at least one zero maximum. First, let us exclude the possibility for existence of positive maxima of φ. Again, we can use (24) but this time let us integrate in the interval $r \in [r_0, r_m]$, where r_m denotes the point at which $\varphi(r)$ has a positive maximum, i.e. $\varphi'(r_m) = 0$. $(\cdot)'$ denotes the derivative with respect to the radial coordinate r. Here r_0 denotes the first zero of φ to the left of r_m. Integrating by parts we get

$$-\int_{r_0}^{r_m} \left[e^{-\delta} r^2 f \left(\frac{d\varphi}{dr}\right)^2\right] dr$$

$$= \int_{r_0}^{r_m} \left\{\varphi \frac{dV(\varphi)}{d\varphi} r^2 + 4r^2 e^{-\delta} \varphi \alpha(\varphi) \mathcal{A}^4(\varphi)[X\partial_X L(X) - L(X)]\right\} dr. \quad (26)$$

Since $\varphi(r)$ is positive in $r \in [r_0, r_m]$ the sign of the RHS of (26) is positive. The LHS, however, is negative. Again we reach a contradiction which means that the admission for presence of a positive maximum of φ is false.

It remains only to exclude the possibility that φ has a maximum and a zero at the same point which we will again denote as r_m. At a zero maximum $\varphi(r_m) = 0$, $\varphi'(r_m) = 0$ and $\varphi''(r_m) < 0$, so from Eq. (18) taking into account also (6) we obtain

$$f\varphi''|_{r_m} = 4\alpha(\varphi)\mathcal{A}^4(\varphi)[X\partial_X L(X) - L(X)]|_{r_m}. \quad (27)$$

The LHS of the above expression is negative while the RHS is positive. This contradiction allows us to exclude the cases of zeros at maxima of φ. This completes the proof of the proposition. □

In our numerical calculations, the following restriction in the behavior of f will be useful.

Proposition 3. *The metric function $f(r)$ cannot have extrema with $f(r) > 1$.*

Proof. Let us consider Eq. (17). Using (20) we can write it in the form

$$1 - f - rf' - r^2 f\varphi'^2 = 2r^2[V(\varphi) - \mathcal{A}(\varphi)^4 L(X)]. \tag{28}$$

From here we obtain

$$-rf' = (f-1) + 2r^2\left[\frac{1}{2}f\varphi'^2 + V(\varphi) - \mathcal{A}(\varphi)^4 L(X)\right]. \tag{29}$$

When $f(r) > 1$ the RHS of (29) is positive so the derivative of $f(r)$ is strictly negative, $f'(r) < 0$. Hence, $f(r)$ cannot have extrema with $f(r) > 1$. □

If we go backwards in r, once it becomes greater than one, $f(r)$ must continue to rise. The inward integration can stop once the point $f(r) = 1$ is surpassed.

Proposition 4. *The metric function $\delta(r)$ is smooth nonincreasing and has inflection points where $\varphi(r)$ has extrema.*

Proof. From Eq. (20) we see that its first derivative is negative so the first part of the proposition is easily proven. Now let us differentiate Eq. (20)

$$\frac{d^2\delta}{dr^2} = -\left(\frac{d\varphi}{dr}\right)^2 - 2r\frac{d\varphi}{dr}\cdot\frac{d^2\varphi}{dr^2}. \tag{30}$$

From (20) and (30) we see that in the extrema of $\varphi(r)$ (the points in which $\varphi'(r) = 0$) $\delta'(r) = \delta''(r) = 0$, i.e. $\delta(r)$ has an inflection point. □

3.3. *Asymptotic solutions*

The presence of potential considerably changes the asymptotic behavior of the scalar field in comparison to the massless scalar field case. In the asymptotic region $r \to \infty$ we find the following behavior for the functions:

$$f(r) = 1 - \frac{2M}{r} + \frac{P^2}{r^2} + \frac{P^4}{40br^6} + \mathcal{O}(r^{-14}), \tag{31}$$

$$\delta(r) = \mathcal{O}(r^{-16}), \tag{32}$$

$$\varphi(r) = -\frac{\alpha(0)P^4}{4m_*^2 br^8} + \mathcal{O}(r^{-9}). \tag{33}$$

These asymptotic solutions are later used as initial approximations for the numerical integration.

3.4. *Units*

In the system of units that we work $G_* = c = \frac{\mu_0}{4\pi} = 1$, where μ_0 is the magnetic constant. In this system

$$[P] = \text{length}; \quad [M] = \text{length}; \quad [m_*] = \text{length}^{-1}; \quad [b] = \text{length}^{-2}.$$

In order to obtain dimensionless quantities we can use the fact that system (20)–(22) is invariant under the rigid re-scaling $r \to \lambda r$, $m \to \lambda m$, $P \to \lambda P$ and $b \to \lambda^{-2} b$, where $0 < \lambda < \infty$. Therefore, from a given solution of (20)–(22) with physical parameters (r_h, M, P, m_*, b, T), the rigid re-scaling produces new solutions with parameters $(\lambda r_h, \lambda M, \lambda P, \lambda^{-1} m_*, \lambda^{-2} b, \lambda^{-1} T)$. Here T denotes the temperature of the horizon. The dimensionless parameters can be obtained through such re-scaling if $[\lambda] = \text{length}^{-1}$. Here, we introduce scale by choosing $\lambda = \sqrt{b}$. Below, we will keep the notation for the dimensionless quantities unchanged.

4. Extremal Solutions

The massive-scalar-field black-hole solution has a much richer causal structure than the one with massless scalar field, since in the former case the presence of an inner horizon and a degenerate event horizon is allowed. Taking into account the conditions for a two-fold degenerate event horizon

$$f(r_e) = 0, \quad \frac{dm(r_e)}{dr} = \frac{1}{2}, \tag{34}$$

and from Eqs. (21) and (22) we obtain

$$r_e^2[V(\varphi_e) - \mathcal{A}^4(\varphi_e) L(X_e)] = \frac{1}{2} \quad , \tag{35}$$

$$r_e^2 \left\{ \frac{dV(\varphi_e)}{d\varphi} - 4\alpha(\varphi_e)\mathcal{A}^4(\varphi_e)[L(X_e) - X_e \partial_X L(X_e)] \right\} = 0. \tag{36}$$

Here and forth r_e will denote the degenerate horizon. Again, subscript "e" denotes the value of the functions evaluated at r_e. Equations (35) and (36) can be solved with respect to r_e^2

$$r_e^2 = \frac{-F_1 \pm \sqrt{F_1^2 - 4\alpha(\varphi_e) F_2}}{2F_2}, \tag{37}$$

where

$$F_1 = \left[\frac{dV(\varphi_e)}{d\varphi} - 4\alpha(\varphi_e) V(\varphi_e) \right], \tag{38}$$

$$F_2 = \left[4b \frac{dV(\varphi_e)}{d\varphi} \mathcal{A}^4(\varphi_e) - 2V(\varphi_e) \frac{dV(\varphi_e)}{d\varphi} + 4\alpha(\varphi_e) V(\varphi_e)^2 \right]. \tag{39}$$

The root for which $0 < r_e^2 < \infty$ for all values of φ_e should be chosen. Then we substitute it in Eq. (35) and obtain the following sophisticated nonlinear

equation for φ_e

$$1 = \frac{-F_1 + \sqrt{F_1^2 - 4\alpha(\varphi_e)F_2}}{2F_2} \times \left\{ 2V(\varphi_e) - 4b\mathcal{A}^4(\varphi_e)\left[1 - \sqrt{1 + \frac{P^2}{2b}\mathcal{A}^4(\varphi_e)\left(\frac{2F_2}{-F_1 + \sqrt{F_1^2 - 4\alpha(\varphi_e)F_2}} \right)^2} \right] \right\}, \tag{40}$$

which we treat numerically for the STT with $\alpha(\varphi) = \text{const.} \equiv \alpha$. The solution for φ_e is substituted back in (37) which, on its turn, gives us the radius of the degenerate horizons. Equation (40) may have two roots for φ_e which give two roots for r_e^2 when substituted back in (37). Which of them describes a degenerate event horizon? Using Eq. (15) we can find the value of f_e'' as

$$f_e'' = -4\{V(\varphi_e) + \mathcal{A}^4(\varphi_e)[2X_e\partial_X L(X_e) - L(X_e)]\}. \tag{41}$$

Hence, we can use the fact that at the degenerate event horizon $f_e'' > 0$ to obtain a criterium which tells us whether the roots of (40) and (37) correspond to a degenerate event horizon. The roots for which $f_e'' < 0$ could correspond to an internal degenerate horizon resulting from the merger of two internal horizons if they existed at all.

Equation (40) for φ_e has two roots. The corresponding values r_{e_1} and r_{e_2} are given in Fig. 1. It should be noted that the analysis for existence of degenerate horizons does not take in consideration the boundary conditions. In other words, it is possible that for some values of the parameters the extremal black-hole solutions are asymptotically nonflat.

From the graphics we see that for fixed values of α and m_*, there is a critical value of the magnetic charge P_{crit}. Solutions with degenerate event horizons exist

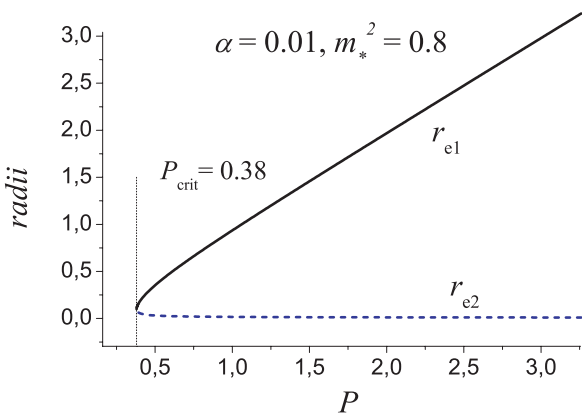

Fig. 1. Solutions for the positions of the degenerate horizons as a function of the magnetic charge P of the black hole.

only for $P > P_{\rm crit}$. For example, when $\alpha = 0.01$ and $m_*^2 = 0.8$, $P_{\rm crit} \approx 0.38$. A degenerate horizon is usually formed when for some values of the black-hole mass M two regular horizons merge. So, it is likely to expect that for $P > P_{\rm crit}$, black holes with two regular horizons exist for some values of M. On the contrary, when $P < P_{\rm crit}$, we should not expect the existence of solution with more than one horizon. Our further numerical investigation confirms the expectations for the case $P > P_{\rm crit}$. We should also note that for fixed $P > P_{\rm crit}$, with the decrease of M, an extremal black hole is reached while for $P < P_{\rm crit}$ — a naked singularity.

The $P-f_e''$ dependence is presented in Fig. 2. As we can see, for the whole interval of its existence, the root r_{e_1} cannot be excluded as a candidate for a degenerate event horizon. The situation with the second root is more complicated. For most values of P, r_{e_2} cannot correspond to a degenerate event horizon. For a small interval close to $P_{\rm crit}$, however, f_e'' is positive. There are several ways to interpret r_{e_2} in that interval. It could correspond to a degenerate internal horizon where the function f has a minimum. Since this analysis does not take into account the boundary conditions at infinity, another possibility would be that this root corresponds to a degenerate event horizon of a black hole with a different asymptotic behavior. The point where f_e'' turns to zero could correspond to a triply degenerate event horizon. Unfortunately, we have not been able to check any of these speculations since the numerical simulations fail in that region of the parameter space.

Alternatively, we could keep the values of α and P fixed, and study the presence of degenerate event horizons for different m_*. The numerical solutions for that case are shown in Fig. 3. A critical value of the scalar-field mass $m_{*,\rm crit}$ appears so that solutions with degenerate event horizons exist only when $m_* > m_{*,\rm crit}$. When $\alpha = 0.01$ and $P = 0.4$, $m_{*,\rm crit} \approx 0.26$. Critical mass $m_{*,\rm crit}$ decreases with the increase of the magnetic charge P.

The m_*-f_e'' dependence is presented in Fig. 4. The comments about the two roots are the same as in the case presented in Fig. 2.

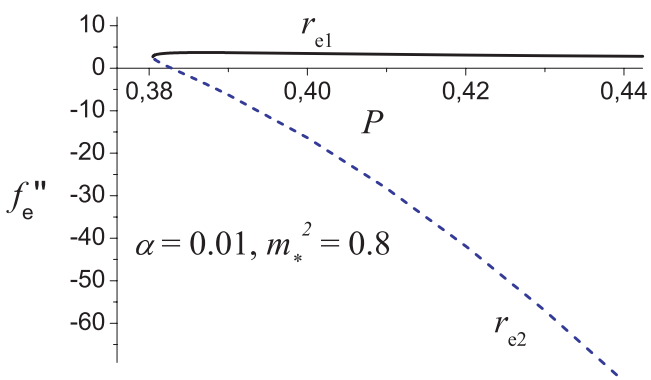

Fig. 2. Derivative f_e'' evaluated on r_{e1} and r_{e2} as a function of the magnetic charge P of the black hole. On a degenerate event horizon $f_e'' > 0$ must hold.

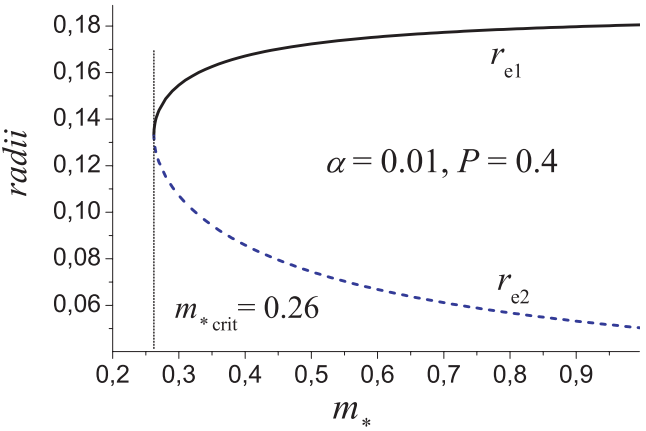

Fig. 3. Solutions for the positions of the degenerate horizons as a function of the scalar field mass m_*.

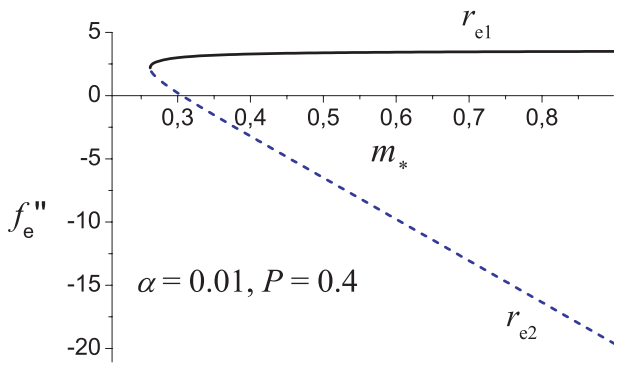

Fig. 4. Derivative f_e'' evaluated on r_{e1} and r_{e2} as a function the scalar field mass m_*. On a degenerate event horizon $f_e'' > 0$ must hold.

The critical value $P_{\rm crit}$ depends on m_* and α. In order to determine this dependence we will use again Eqs. (35) and (36). Let us introduce a new variable

$$k = \sqrt{1 + \frac{X_e}{b}}. \tag{42}$$

The variable k can be expressed as a function of φ_e from (36). Using (3.1) and (42) we can express r_e^2 in the following way:

$$r_e^2 = \frac{\mathcal{A}^{-2}(\varphi_e)|P|}{\sqrt{2}\sqrt{k^2-1}}. \tag{43}$$

Then, in (35) we express $L(X_e)$ with k and r_e^2 from (43). Introducing a new variable $y = \alpha\varphi_e$, we obtain

$$\frac{1}{2} = \sqrt{2}|P|\frac{\gamma y^2 e^{-2y} + e^{2y}(k-1)}{\sqrt{k^2-1}} = \sqrt{2}|P|F(y,\gamma), \tag{44}$$

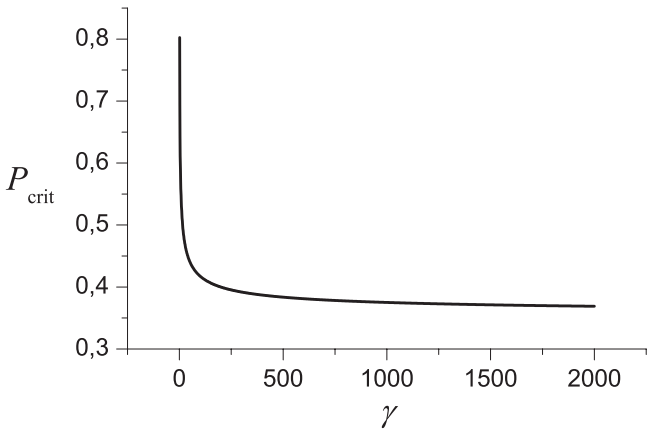

Fig. 5. The $\gamma - P_{\text{crit}}$ critical curve.

where

$$\gamma = \frac{m_*^2}{4\alpha^2}.$$

In (44) there are two free parameters $|P|$ and γ. Let us fix the value of γ. Then $F(y, \gamma)$ has one maximum ($y < 0$). Depending on $|P|$ the RHS of (44) can be greater, equal to or less than the LHS, and the equations have, respectively, two, one, or no solutions. So P_{crit} is the value for which (44) has only one solution.[d] The $\gamma - P_{\text{crit}}$ critical curve is plotted in Fig. 5.

5. Numerical Integration

The nonlinear system (20)–(22) is inextricably coupled. Our aim is to obtain numerical solutions that describe asymptotically flat black holes. We split the problem in two boundary sub-problems — in the exterior and in the interior region of the black hole, which we solve subsequently.

5.1. *External problem*

First, let us consider the exterior region. For that region we can formulate a boundary value problem (BVP) for (20)–(22) with the boundary conditions

$$\lim_{r\to\infty} m(r) = M \quad (M \text{ is the mass of the black hole in the Einstein frame}),$$
$$\lim_{r\to\infty} \delta(r) = \lim_{r\to\infty} \varphi(r) = 0,$$

[d] P is non-negative.

for the right-hand boundary at spatial infinity and

$$f(r_H) = 0$$

on the horizon. The left-hand boundary, namely the event horizon, is *a priori* unknown. Such BVPs are known in mathematical physics as BVPs of Stefan kind (see, for example, Ref. 49). For the location of the event horizon an additional condition is needed. It can come from the requirement that all functions are to be regular on the event horizon

$$\left(\frac{df}{dr}\cdot\frac{d\varphi}{dr}\right)\Big|_{r=r_H} = \frac{dV(\varphi)}{d\varphi}\Big|_{r=r_H} + \left\{4\alpha(\varphi)\mathcal{A}^4(\varphi)[X\partial_X L(X) - L(X)]\right\}\Big|_{r=r_H}.$$

We can also think of the so formulated BVP as a nonlinear analogue of a spectral problem with regard to parameter r_H.

Having in mind these features of the above posed BVP, we treat it by applying the continuous analog of Newton method (see, for example, Refs. 40, 50 and 51). After an appropriate linearization, the original BVP is rendered to solving standard vector two-point BVPs. On a discrete level, almost diagonal linear algebraic systems with regard to increments of sought functions $\delta(r)$, $m(r)$ and $\varphi(r)$ have to be inverted.

5.2. *Internal problem*

The exterior solutions can be continued inward. The values of the functions and their derivatives on the event horizon are obtained *a priori* in the exterior problem. This allows an initial-value problem (IVP) for the same system (20)–(22) to be formulated in the interior region $r < r_H$ *a posteriori*. The event horizon, however, is a singular point for the equation of the scalar field (22) since the coefficient in front of φ'' turns to zero there ($f(r_H) \equiv 0$) and the equation loses its leading order term. So, to pose a regular IVP, we shift the initial point r_H by small enough $\varepsilon > 0$ and choose for initial point $r_H - \varepsilon$ instead r_H. On the other hand, the functions in question are smooth in the interval $(r_H - \varepsilon, r_H)$ and hence the following series expansions hold:

$$m(r_H - \varepsilon) = m(r_H) - m'(r_H)\varepsilon + o(\varepsilon^2), \tag{45}$$

$$\delta(r_H - \varepsilon) = \delta(r_H) - \delta'(r_H)\varepsilon + o(\varepsilon^2), \tag{46}$$

$$\varphi(r_H - \varepsilon) = \varphi(r_H) - \varphi'(r_H)\varepsilon + o(\varepsilon^2), \tag{47}$$

$$\Phi(r_H - \varepsilon) = \Phi(r_H) - \Phi'(r_H)\varepsilon + o(\varepsilon^2), \quad \text{where } \Phi(r) = \varphi'(r). \tag{48}$$

A similar shift is made whenever an inner horizon is reached. The latter admits an algorithmic sequence of IVPs for finding possible inner horizons. For the numerical treating of the above posed IVP, again we apply the continuous analog of Newton method.

5.3. *Some results*

Let us first consider the case $P > P_{\rm crit}$. The numerical investigation of the solutions shows that for fixed values α and m_*, the general structure of the solutions depends strongly on the charge-to-mass ratio P/M. For low enough P/M, the obtained black-hole solutions have a single horizon, namely the event horizon. For high enough P/M, (for P/M close to 1) the black holes have two horizons or one degenerate horizon (an extremal solution is reached when we decrease the mass M and keep P fixed).

Two examples of solutions with a single horizon are shown (the functions f, δ and φ, respectively) in Figs. 6–8. The values of the parameters in the presented examples are: $\alpha = 0.01, m_*^2 = 0.8, P = 6.0$ and two different masses of the black hole $M = 21.5$ and $M = 25.0$. As it can be seen in Fig. 6 for $M = 21.5$, the function

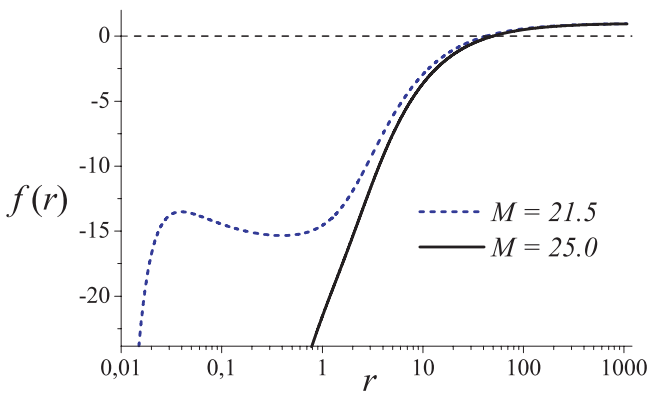

Fig. 6. The metric function f for $\alpha = 0.01, m_*^2 = 0.8, P = 6.0$ and two different masses of the black hole $M = 21.5$ and $M = 25.0$. The abscissa is in logarithmic scale.

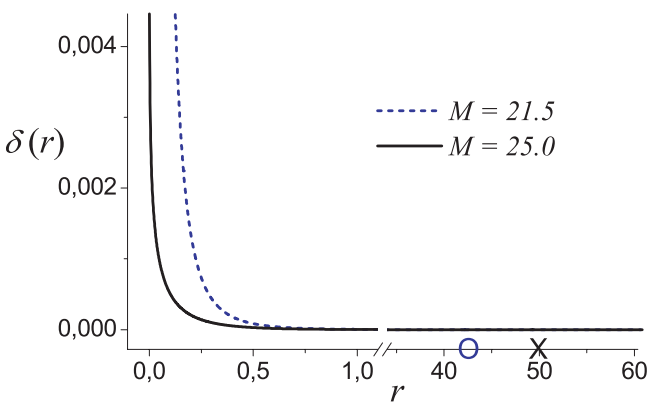

Fig. 7. The metric function δ for $\alpha = 0.01, m_*^2 = 0.8, P = 6.0$ and two different masses of the black hole $M = 21.5$ and $M = 25.0$.

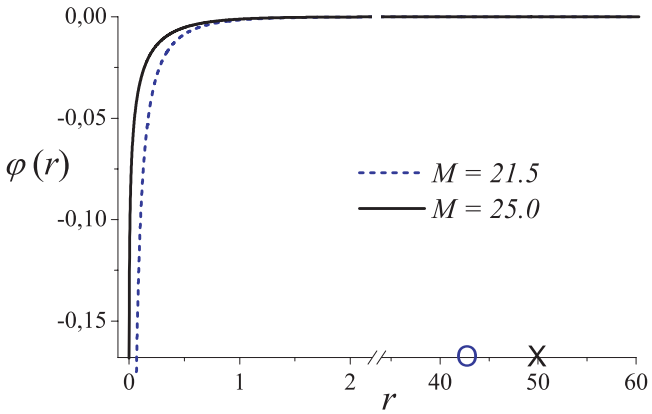

Fig. 8. The scalar field φ for $\alpha = 0.01, m_*^2 = 0.8, P = 6.0$ and two different masses of the black hole $M = 21.5$ and $M = 25.0$.

f has negative extrema below the event horizon (the abscissa in that figure is in logarithmic scale). In Figs. 7 and 8, the radius of the solution with $M = 21.5$ is designated with "◯" and for $M = 25.0$ with "×."

Solutions with two horizons and with one degenerate horizon are given in Figs. 9–11. The values of the parameters in these cases are $\alpha = 0.01, m_*^2 = 0.8$, $P = 6.0$, and black-hole masses $M = 5.9804$ for the extremal black hole and $M = 8.0$ for the black hole with two horizons. We can see that in accordance with our observations from Sec. 3, $\delta(r)$ has an inflection point in the extremum of $\varphi(r)$. In Figs. 10 and 11, the radius of the extremal black hole is designated with "◯" while the two radii of the solution with $M = 8.0$ are designated with "×"-es.

The presence of numerical instabilities did not allow us to study thoroughly the interior region for the case $P < P_{\text{crit}}$.

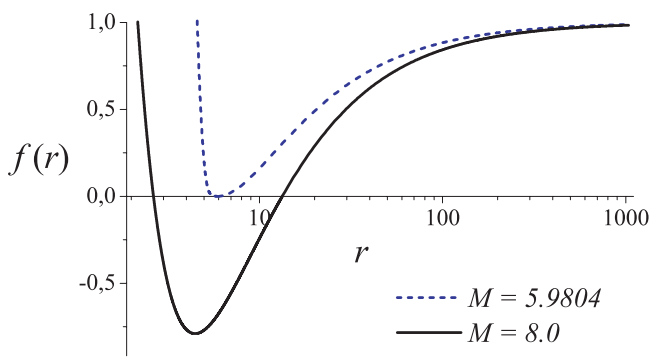

Fig. 9. The metric function f for $\alpha = 0.01, m_*^2 = 0.8, P = 6.0$ and two different masses of the black hole $M = 5.9804$ and $M = 8.0$. The abscissa is in logarithmic scale.

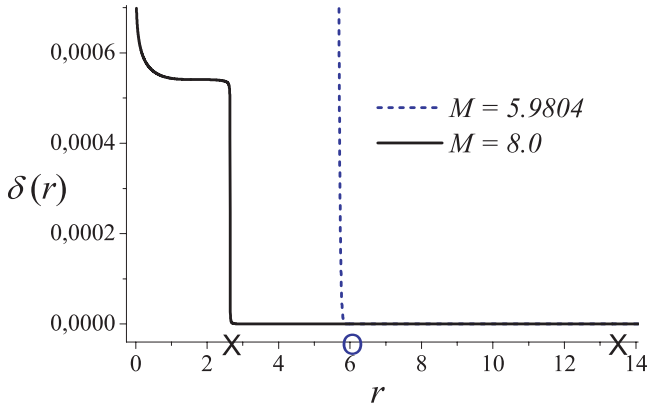

Fig. 10. The metric function δ for $\alpha = 0.01, m_*^2 = 0.8, P = 6.0$ and two different masses of the black hole $M = 5.9804$ and $M = 8.0$.

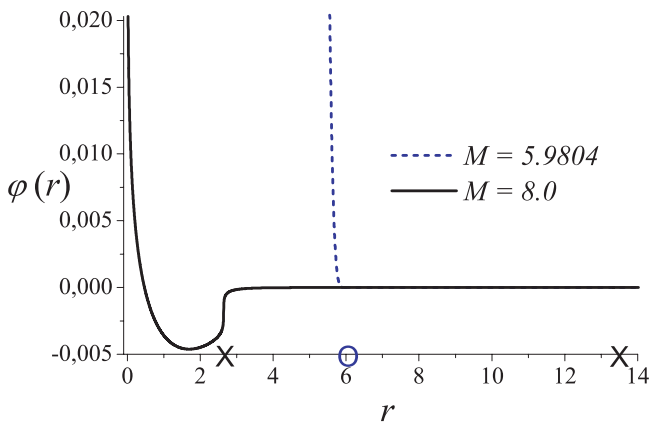

Fig. 11. The scalar field φ for $\alpha = 0.01, m_*^2 = 0.8, P = 6.0$ and two different masses of the black hole $M = 5.9804$ and $M = 8.0$.

6. Thermodynamics

Since the entropy of the black hole is related to the area and, respectively, to the radius of the event horizon, in Figs. 12 and 13 we have given the $M{-}r_H$ and the $P{-}r_H$ diagrams. In the presented cases, $\alpha = 0.01$ and $m_*^2 = 0.8$. For these values of the parameters, $P_{\rm crit} \approx 0.38$. We have given two graphics — one for $P = 6.0 > P_{\rm crit}$ and one for $P = 0.3 < P_{\rm crit}$. In the former case, for masses in the interval $M \in [5.9804, 21.1]$, the black holes have two regular horizons (in Fig. 12 they are designated as *event horizon* and *inner horizon*). The two horizons merge and an extremal black hole occurs at $M = 5.9804$. The value of event horizon obtained through numerical integration of the equations and the one obtained through solution of the algebraic problem in Sec. 4 coincide within the approximation and

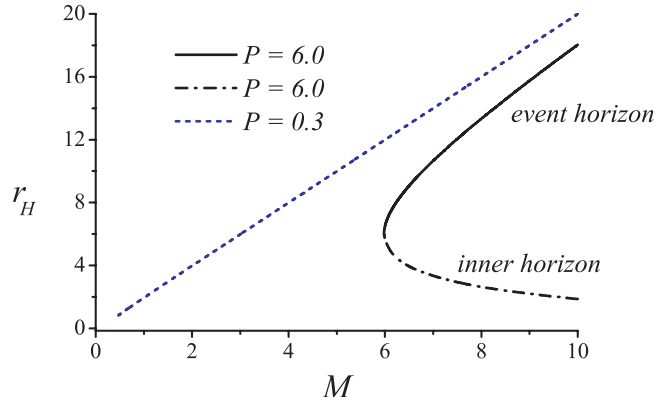

Fig. 12. The radii of the horizons of black holes as a function of the mass M. For $P = 6$, the black hole has two horizon — event horizon and inner horizon. For $P = 0.3$ the black holes have a single horizon — the event horizon.

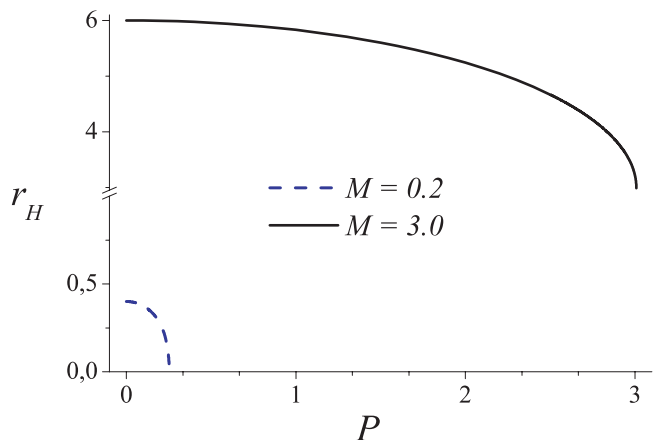

Fig. 13. The $r_H - P$ relation.

round-off error which is a very good test for the correctness of the obtained numerical results. In the latter case, the black holes have a single, non-degenerate horizon.

Let us try to obtain some intuition of the general behavior of our solutions through comparison to the solution of Reissner–Nordström (RN). In RN, black holes exist for $M \geq P$. An extremal black hole occurs at $P/M = 1$. Similarly, in our case, from the $M - r_H$ relation (12) we see that, black-hole solutions exist for $M \geq P$. Unlike RN, however, in our case black holes exist also for M a bit less than P but still the extremal black hole occurs at P/M close to 1. So if we fix the value of M, the maximal value of P is of the same order. We can also define M_{crit} as the mass of the extremal black hole when $P = P_{\text{crit}}$. The relation $P_{\text{crit}}/M_{\text{crit}} \approx 1$ also holds. This dependence can be also seen in Fig. 13 where the $P - r_H$ relation is

shown.[e] Let us set $M = 0.2$. Then according to our admission, P cannot be much greater than 0.2 so it will be less than $P_{\rm crit}$. Indeed, from Fig. 13 we see that, in that case a naked singularity is reached when P approaches its maximal value (see the comments at the end of Sec. 4). For $M = 3.0$ an extremal black hole appears when P approaches its maximal value.

A knowledge about the general stability of the obtained solutions can be obtained through the application of the so-called "turning point" method (we refer the reader to Refs. 52–55 for a detailed discussion on the "turning point" method and also to Refs. 39, 43 and 56 for the application of the method to study the thermodynamical stability of black holes). According to that method, in micro-canonical ensemble,[f] a change of the stability reveals itself on the $M{-}T^{-1}$ diagram as a bifurcation or as a turning point. Here "bifurcation point" is used to denote a point where brunching of equilibrium sequences occurs, while a "turning point" is such point where two equilibrium sequences merge with a vertical tangent. The absence of such points on the $M{-}T^{-1}$ diagram means that if at least one point on the equilibrium sequence is stable, then the whole equilibrium sequence is stable.

The $M{-}T^{-1}$ diagram for the studied solutions is given in Fig. 14. Again we present the two cases, $P = 6.0 > P_{\rm crit}$ and $P = 0.3 < P_{\rm crit}$. In both of them, when M is large, $T^{-1} \approx M$, i.e. the solutions approach the Schwarzschild black hole.[g] The stability of the Schwarzschild black hole within the theory of Brans–Dicke has already been proved,[57] so we expect that for large M our solutions are stable. Since in both of the presented cases no turning or bifurcation point appears on the diagram, we can expect that the entire equilibrium brunches are stable. With the decrease of M, the inverse temperature T^{-1} of the solutions with $P > P_{\rm crit}$ increases

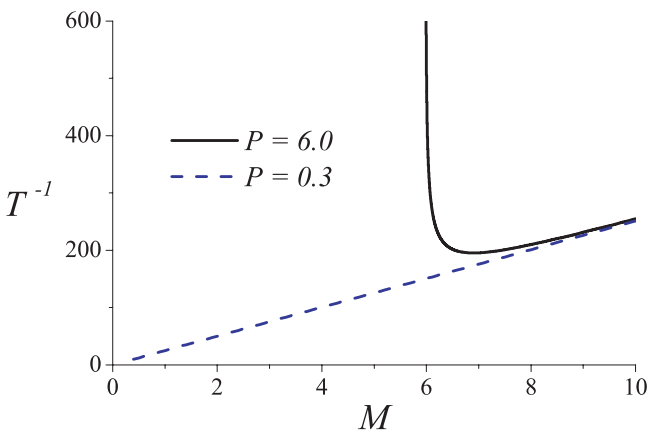

Fig. 14. The $M{-}T^{-1}$ relation.

[e]In that figure only the radii of the event horizons are shown.
[f]We keep the magnetic charge P of the black hole fixed.
[g]For the Schwarzschild black hole $T^{-1} = M$.

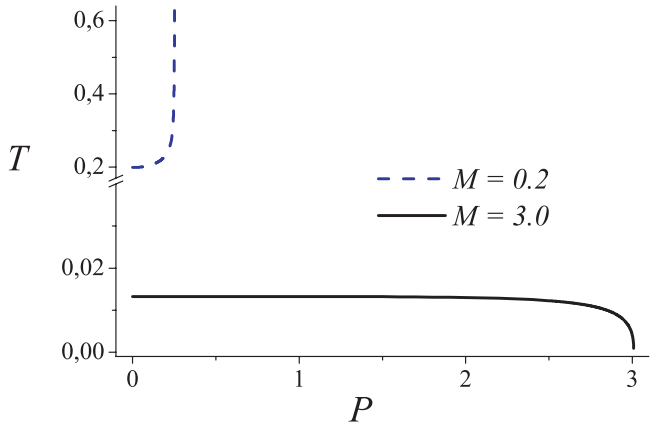

Fig. 15. The $P-T$ relation.

unboundedly since an extremal solution is reached, while for $P < P_{\rm crit}$, T^{-1} goes to zero since an object with zero radius of the horizon, i.e. a naked singularity, is reached. In Fig. 15 the $P-T$ relation is shown. For $M > M_{\rm crit}$, an extremal black hole is reached with the increase of P so the temperature of the horizon goes to zero. For $M < M_{\rm crit}$, a naked singularity is reached with the increase of P and the temperature of the horizon rises unboundedly.

7. Stability of the Solutions Against Spherically Symmetric Perturbations

7.1. *Stability of the magnetically charged black holes*

In order to examine the stability of the solutions against radial perturbations, we apply the scheme presented in detail in Ref. 43. First, we establish the stability against radial perturbations of the magnetically charged solutions. Then, we study the electrically charged case through the electric–magnetic duality rotations. We use the following ansatz for the metric of a spherically symmetric, time-dependent spacetime:

$$ds^2 = -e^{\gamma}dt^2 + e^{\chi}dr^2 + e^{\beta}(d\theta^2 + \sin^2\theta d\phi^2), \tag{49}$$

where γ, χ and β are functions of r and t. The perturbed fields are presented in the following way:

$$\begin{aligned} &\gamma(r,t) = [-2\delta(r) + \ln f(r)] + \triangle\gamma(r,t), \quad \chi(r,t) = -\ln f(r) + \triangle\chi(r,t), \\ &\beta(r,t) = 2\ln r + \triangle\beta(r,t), \quad \varphi(r,t) = \varphi(r) + \triangle\varphi(r,t), \end{aligned} \tag{50}$$

where $\delta(r)$, $f(r)$ and $\varphi(r)$ give the static background solution, and $\triangle\gamma(r,t)$, $\triangle\chi(r,t)$, $\triangle\beta(r,t)$ and $\triangle\varphi(r,t)$ are small time-dependent perturbations. Let us impose the convenient gauge $\triangle\beta(r,t) = 0$. Then e^{β} simply reduces to r^2.

In the case of spherically symmetric perturbations, the equations decouple and the system reduces to a single equation for the perturbations of the scalar field

$$\nabla^{(0)}_{\mu}\nabla^{(0)\mu}\triangle\varphi - U(r)\triangle\varphi = 0, \tag{51}$$

where

$$\begin{aligned} U(r) = &-2\{1-2r^2[V-\mathcal{A}^4(\varphi)L(X)]\}[\partial_r\varphi(r)]^2 + 4r[\partial_r\varphi(r)]\frac{dV}{d\varphi} + \frac{d^2V}{d\varphi^2} \\ &+ \mathcal{A}^4(\varphi)[16r\partial_r\varphi(r)\alpha(\varphi) + 4\partial_\varphi\alpha(\varphi)][X\partial_X L(X) - L(X)] \\ &- 16\alpha^2(\varphi)\mathcal{A}^4(\varphi)[X^2\partial^2_X L(X) - X\partial_X L(X) + L(X)], \end{aligned} \tag{52}$$

and $\nabla^{(0)}_{\mu}$ is the co-derivative operator with respect to the static background. Since the background solution is static, Eq. (51) admits a separation of the variables. Using the following substitution:

$$\triangle\varphi(r,t) = \psi(r)e^{i\omega t}, \tag{53}$$

from (51) we obtain an equation for the spacial part of the perturbations

$$f(r)e^{-\delta(r)}\frac{d}{dr}\left[f(r)e^{-\delta(r)}\frac{d\psi}{dr}\right] + \frac{2}{r}f^2(r)e^{-2\delta(r)}\frac{d\psi}{dr} + \omega^2\psi = f(r)e^{-2\delta(r)}U(r)\psi, \tag{54}$$

where ω^2 acts as a spectral parameter. Equation (54) can be cast in the form of Schrödinger equation. In order to do this, we will use the tortoise radial coordinate r_* and a proper substitution for ψ

$$dr_* = \frac{dr}{f(r)e^{-\delta(r)}}, \quad \psi(r) = \frac{u(r)}{r}. \tag{55}$$

The following Schrödinger-like equation:

$$\frac{d^2u(r_*)}{dr_*^2} + \omega^2 u(r_*) = U_{\text{eff}}(r_*)u(r_*), \tag{56}$$

is reached. The effective potential is

$$U_{\text{eff}}(r_*) = f(r_*)e^{-2\delta(r_*)}\left\{U(r_*) - 2V(\varphi) + 2\mathcal{A}^4(\varphi)L(X) + \frac{1}{r^2(r_*)}[1-f(r_*)]\right\}. \tag{57}$$

For r varying in the interval $[r_H, \infty)$, where r_H is the radius of the event horizon, the tortoise radial coordinate $r_* \in (-\infty, \infty)$. From this point we can use the techniques from the standard quantum mechanics to study the properties of the small perturbations.

In the numerically studied region of the parameter space, the effective potential U_{eff} is nonnegative which means that the studied black holes are stable against spherically symmetric perturbations. Two illustrative cases are given in Fig. 16 for $\alpha = 0.01$, $m_*^2 = 0.8$, $P = 6.0$ and two values of the black-hole mass: $M = 10.0$, for which the black hole has a regular event horizon, and $M = 5.98$ corresponding to an extremal black hole. Here we should note that in the figure, the effective potential

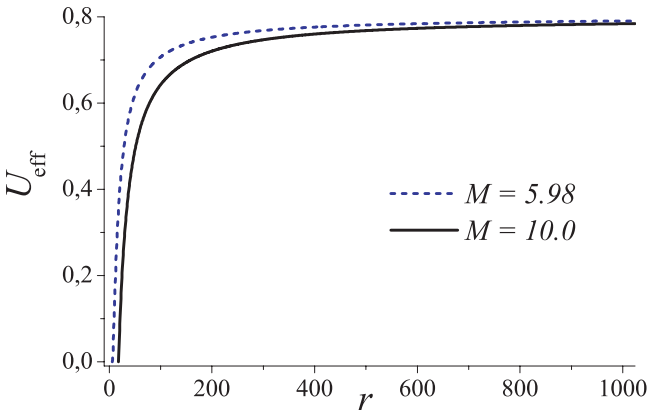

Fig. 16. The effective potential U_{eff} for $\alpha = 0.01$, $m_*^2 = 0.8$, $P = 6.0$ and two values of the black-hole mass $M = 10.0$, for which the black hole has a regular event horizon, and for $M = 5.98$ corresponding to an extremal black hole.

is presented in terms of the radial coordinate, r. In terms of the tortoise coordinate, U_{eff} would be more stretched but still nonnegative.

7.2. *Stability of the electrically charged black holes*

The perturbations of the fields in the electrically charged case can be obtained from the magnetically charged case through the electric–magnetic duality rotations. These transformations preserve the functions of the metric and the scalar field. The perturbations of the electromagnetic field, however, will be nonvanishing in the electrically charged case. For them the duality rotations give (see Ref. 43)

$$\triangle \bar{F}_{\mu\nu} = \frac{1}{2}(\star G)_{\mu\nu}(\triangle\chi + \triangle\gamma) + 4\alpha(\varphi)X\partial_X^2 L(X)(\star F)_{\mu\nu}\triangle\varphi - \partial_X L(X)(\star\triangle F)_{\mu\nu}. \tag{58}$$

Thus, the perturbations of the electromagnetic field can be expressed in terms of the functions of the background, static solution and the perturbations of the magnetically charged solution. So the perturbations of the electrically charged solution will remain bounded with time as long as the perturbations of the magnetically charged solution are.

8. Summary and Discussion

In the present work, numerical solutions describing charged black holes coupled to nonlinear electrodynamics in the STTs with massive scalar field were found. Since an electric–magnetic duality is present in the used electrodynamics, only purely magnetically case was studied here. For the Lagrangian of the nonlinear electrodynamics the truncated Born–Infeld Lagrangian was chosen and STT with massive scalar field and positive coupling parameter were considered. As a result of

the numerical and analytical investigations, some general properties of the solutions were found. The analytical investigations show that the scalar field φ is nonpositive in the exterior region of the black hole. The metric function f cannot have extrema when $f > 1$. The last result can serve as a stop condition for the inward integration. The metric function δ has inflection points at the extrema of φ. All this analytic results for the qualitative behavior of the functions have been confirmed by the numerics.

The causal structure of the black holes has been studied numerically. A critical value of the magnetic (electric) charge $P_{\rm crit}$ was found. When $P < P_{\rm crit}$, the causal structure of the black holes reported here is similar to that of the charged, scalar–tensor black holes with massless scalar field.[41] They have a single, nondegenerate horizon.

When $P > P_{\rm crit}$, the causal structure of the charged, scalar–tensor black holes with massive scalar field presented in the current paper resembles that of the EBI black hole. For $M \gg P$ the black holes have, again, a single nondegenerate event horizon. With the decrease of the mass, a second, inner horizon occurs and finally an extremal black hole is reached. Unlike the RN black hole, here the extremal value of M is a bit lower than the magnetic charge P.

We have also found that the value of $P_{\rm crit}$ depends strongly on γ (see Fig. 5).[h] In the limit $\gamma \to 0$, the critical charge $P_{\rm crit}$ is shifted to infinity and the structure of the present solutions approaches that of the charged, scalar–tensor black holes with massless scalar field. While for large γ, the structure of the present solutions approaches that of the EBI black hole. For the considered values of m_* and α, which have been chosen to be in agreement with the observational constraints, the graphics of the charged, scalar–tensor black holes with massive scalar field are hardly distinguishable from those of the EBI black holes and those of the charged, scalar–tensor black holes with massless scalar field.

It appears that the inclusion of mass for the scalar field does not change the stability of the black holes. The obtained black holes are stable against radial perturbations. The analysis based on the "turning point" implies global stability.

Acknowledgments

This work was partially supported by the Bulgarian National Science Fund under Grants VUF-201/06, DO-02-257, Sofia University Research Fund No. 074/2009 and Technical University Sofia Grant 091ni143-11/2009.

References

1. M. Born and L. Infeld, *Proc. R. Soc. London A* **143** (1934) 410.
2. E. Fradkin and A. Tseytlin, *Phys. Lett. B* **163** (1985) 123.
3. E. Bergshoeff, E. Sezgin, C. Pope and P. Townsend, *Phys. Lett. B* **188** (1987) 70.

[h]The re-scaled critical charge of the EBI is $P_{\rm crit} = 0.5$.

4. R. Metsaev, M. Rahmanov and A. Tseytlin, *Phys. Lett. B* **193** (1987) 207.
5. R. Leigh, *Mod. Phys. Lett. A* **4** 2767 (1989).
6. A. García, H. Salazar and J. Plebañski, *Nuovo Cimento Soc. Ital. Fis. B* **84** (1984) 65.
7. M. Demianski, *Found. Phys.* **16** (1986) 187.
8. D. Wiltshire, *Phys. Rev. D* **38** (1988) 2445.
9. H. P. Oliveira, *Class. Quantum Gravity* **11** (1994) 1469.
10. G. Gibbons and D. Rasheed, *Nucl. Phys. B* **454** (1995) 185.
11. G. Gibbons and D. Rasheed, *Phys. Lett. B* **476** (1996) 515.
12. E. Ayon-Beato and A. Garcia, *Phys. Rev. Lett.* **80** (1998) 5056.
13. T. Tamaki and T. Torii, *Phys. Rev. D* **62** (2000) 061501R.
14. M. Novello, S. Perez Bergliaffa and J. Salim, *Class. Quantum Gravity* **17** (2000) 3821.
15. K. Bronnikov, *Phys. Rev. D* **63** (2001) 044005.
16. G. Gibbons and C. Herdeiro, *Class. Quantum Gravity* **18** (2001) 1677.
17. H. Yajima and T. Tamaki, *Phys. Rev. D* **63** (2001) 064007.
18. M. Gurses and O. Sarioglu, *Class. Quantum Gravity* **20** (2003) 351.
19. A. Burinskii and S. R. Hildebrandt, *Phys. Rev. D* **65** (2002) 104017.
20. S. Fernando and D. Krug, *Gen. Relativ. Gravit.* **35** (2002) 129.
21. T. Dey, *Phys. Lett. B* **595** (2004) 484.
22. T. K. Dey, *Phys. Lett. B* **595** (2004) 484.
23. I. Stefanov, S. Yazadjiev and M. Todorov, *Mod. Phys. Lett. A* **22**(17) (2007) 1217.
24. D. Rasheed, arXiv:hep-th/9702087.
25. N. Breton, arXiv:gr-qc/0109022.
26. N. Breton, arXiv:hep-th/0702008.
27. R. Cai, D. Pang and A. Wang, *Phys. Rev. D* **70** (2004) 124034, arXiv:hep-th/0410158.
28. T. Tamaki, *J. Cosmol. Astropart. Phys.* **0405** (2004) 004.
29. G. Clement and D. Gal'tsov, *Phys. Rev. D* **62** (2000) 124013.
30. T. Tamaki and T. Torii, *Phys. Rev. D* **64** (2001) 024027.
31. S. Yazadjiev, *Phys. Rev. D* **72** (2005) 044006.
32. A. Sheykhi, N. Riazi and M. H. Mahzoon, *Phys. Rev. D* **74** (2006) 044025.
33. A. Sheykhi and N. Riazi, *Phys. Rev. D* **75** (2007) 024021.
34. T. W. Chemissany, Mees de Roo and S. Panda, *Class. Quantum Gravity* **25** (2008) 225009.
35. A. Sheykhi, *Phys. Lett. B* **662** (2008) 7.
36. A. Sheykhi, arXiv:0801.4112.
37. R. Gregory and J. A. Harvey, *Phys. Rev. D* **47** (1993) 2411.
38. J. Horne and G. Horowitz, *Nucl. Phys. B* **399** (1993) 169.
39. T. Tamaki, *Phys. Rev. D* **66** (2002) 104021.
40. S. Yazadjiev, P. Fiziev, T. Boyadjiev and M. Todorov, *Mod. Phys. Lett. A* **16** (2001) 2143.
41. I. Stefanov, S. Yazadjiev and M. Todorov, *Phys. Rev. D* **75** 084036 (2007).
42. I. Stefanov, S. Yazadjiev and M. Todorov, *Mod. Phys. Lett. A* **23**(34) (2008) 2915, arXiv:0708.4141.
43. I. Stefanov, S. Yazadjiev and M. Todorov, *Class. Quantum Gravity* **26** (2009) 015006.
44. N. Banerjee and S. Sen, *Phys. Rev. D* **47** (1998) 104024.
45. Th. Sotiriou, V. Faraoni and St. Liberati, *Int. J. Mod. Phys. D* **17** (2008) 399.
46. V. Faraoni and Sh. Nadeau, *Phys. Rev. D* **75** (2007) 023501.
47. Th. Helbig, *Astrophys. J.* **382** (1991) 223.
48. C. M. Will, *Living Rev. Relativ.* **9** (2006) 3, arXiv:gr-qc/0103036.

49. A. N. Tikhonov and A. A. Samarskii, *Equations of Mathematical Physics* (Nauka, Moscow, 1990) (in Russian) (English translation: Dover Publications, New York, 1990).
50. M. K. Gavurin, *Izvestia VUZ, Matematika* **14**(6) (1958) 18–31 (in Russian) [see also *Math. Rev.* **25**(2) (1963) 1380].
51. E. P. Jidkov, G. I. Makarenko and I. V. Puzynin, in *Physics of Elementary Particles and Atomic Nuclei* ((Joint Institute for Nuclear Research (JINR)), Dubna, 1973), Vol. 4, Part I, pp. 127–166 (in Russian), English translation: *American Institute of Physics*, p. 53.
52. J. Katz, *Mon. Not. R. Astron. Soc.* **183** (1978) 765.
53. R. Sorkin, *Astrophys. J.* **249** (1981) 254.
54. R. D. Sorkin, *Astrophys. J.* **257** (1982) 847.
55. G. Arcioni and E. Lozano-Tellechea, *Phys. Rev. D* **72** (2005) 104021.
56. J. Katz, *Mon. Not. R. Astron. Soc.* **189** (1979) 817.
57. O. J. Kwon, Y. D. Kim, Y. S. Myung, B. H. Cho and Y. J. Park, *Phys. Rev. D* **34** (1986) 333.
58. T. Torii, T. Tamaki and K. Maeda, *Phys. Rev. D* **68** (2003) 024028.